Third International Conference on Multidisciplinary
Design Optimization and Applications,
June 21-23, 2010 Paris, France
www.asmdo.com/conference2010/

# Analysis of the pull-in voltage in capacitive mechanical sensors

Joseph Lardiès, Olivia Arbey and Marc Berthillier

*University of Franche-Comté, FEMTO-ST Institute, DMA,*
*24, rue de l'Epitaphe, 25000 Besançon, France*
joseph.lardies@univ-fcomte.fr

**Abstract**
*MEMS based capacitive type sensors offer advantages due to their small size, relative high sensitivity, batch fabrication capability, low power consumption and low noise features. A MEMS capacitive sensor is basically an electrostatic transducer and an analytical approach is used to model a MEMS-based capacitive-type sensor. A closed-form model to evaluate the pull-in voltage associated with a clamped square diaphragm and a circular diaphragm subject to electrostatic forces due to a bias voltage is developed. The approach is based on a linearized uniform approximation of the nonlinear electrostatic force due to the bias voltage and the use of a 2D load deflection model for MEMS based capacitive acoustical sensor. The spring hardening effect associated with nonlinear stretching of the central region of a clamped diagram is also considered. The resulting electrostatic pressure on the diaphragm, the pull-in voltage, and the deflection of the midpoint of the diaphragm for different bias voltage are studied. A comparison of the results obtained using the developed analytical model of the communication with the results obtained by Senturia is discussed. Numerical results are presented showing the effectiveness of the method in nonlinear identification problems.*

## 1 Introduction

Any micro-electro-mechanical system (MEMS) includes input transducers, mechanical resonators and output transducers. The input transducers convert the input electrical signals into an electrical force. The force acting on mechanical resonators sufficiently isolated from their surroundings causes the corresponding vibration of the resonators. The output transducers will sense the motion of the mechanical resonator and generate the corresponding electrical signals. The central component in micro-electro-mechanical systems is the mechanical resonator which constitutes a capacitive transducer and is formed with two plates: a fixed plate and a movable plate. Due to the electrical force, when the gap between the two plates becomes two thirds of the initial gap, the movable plate is not stable, we have a ''push-down'' phenomenon and the MEMS fails. From the dynamics point of view, the system loses its stability. The gap being equal to two-thirds of the initial gap is termed the minimum gap in MEMS [1]. In fact, stoppers are used in the design of MEMS for avoiding such a failure of the capacitor. The main function of MEMS is to transfer input signals to output signals with a specific frequency

relationship through a mechanical resonator. If the exact frequency of MEMS cannot be determined, the vibration of mechanical resonator in MEMS cannot be easily induced by input signals with certain frequencies. Furthermore, the output signals cannot be sensed out, which leads to the failure of MEMS. Due to the enormous advance in microelectronics and signal processing, small size, bandwidth, high sensibility, low power consumption and batch fabrication, MEMS capacitive sensors, usually called CMUT (capacitive micromachined ultrasonic transducer) have been an attractive alternative to conventional piezoelectric transducers in the generation and detection of ultrasound in air and water. The CMUT is constructed directly on a silicon substrate by means of CMOS technology and provides the advantage of increased bandwidth with comparable sensitivity to conventional piezoelectric transducers as well as ease of fabrication and electronics integration. The CMUT consists of a lot of very thin square or circular silicon nitride membranes in parallel suspended above silicon substrate. Basically, the single cell of a CMUT is an electrostatic transducer like the well known condenser microphone [1]; nevertheless, this kind of capacitive transducer is able not only to detect but also to generate acoustic waves in fluids. This capacitive-type sensor is then basically an electrostatic transducer that depends on electrical energy in terms of constant voltage (voltage drive) to facilitate monitoring of capacitance change due to an external mechanical excitation such as force or acoustical pressure. The electrostatic force associated with the voltage is non linear due to its inverse square relationship with the airgap thickness between the capacitor electrodes. This gives rise to a phenomenon known as ''pull-in'' that causes the movable structure (membrane) to collapse if the bias voltage exceeds the pull-in limit and limits the effective range of deformation of the structure. Accurate determination of the pull-in voltage, or the collapse voltage, is critical in the design process to determine the sensitivity, harmonic distortion and the dynamic range of a MEMS-based capacitive transducer with a square or a circular diaphragm. Pull-in instability is fundamental to the understating of many MEMS devices and is one of the basic parameters of the design of many electrostatic MEMS devices. Lack of an accurate model for predicting pull-in voltage for basic beam structures such as fixed-fixed beams, fixed-free beams or for basic membranes necessitates the clear need for a closed form expression for the pull-in voltage. Attempts have been made by several authors in the past [1-4] to derive a closed-form expression for the pull-in voltage.

In this communication an analytical solution is presented to calculate the pull-in voltage and diaphragm deflection for a clamped square diaphragm and a circular clamped diaphragm under electrostatic actuation. The method includes the nonlinearities of the electrostatic force and the large deflection model for a clamped square and a clamped circular diaphragm deflection.

## 2 The model

The basic structure of a MEMS capacitive microphone is shown in Figure 1 : a metalized membrane stretched by a tensile force is put in front of a fixed conducting backplate by means of a surrounding border which assures a separation distance. In fact, the structure can be viewed as a parallel plate capacitor consisting of a top diaphragm and a bottom backplate separated by a small airgap acting as the dielectric material. When an acoustical sound wave is incident on the diaphragm, it causes the diaphragm to deflect and the gap between the diaphragm and the backplate decreases causing an increase in the capacitance between them. As the diaphragm vibrates in accordance with the frequency of the acoustical wave, the capacitance between the electrodes changes accordingly due to a variable airgap. If a battery is connected across the diaphragm and the backplate, following the principle of energy conservation, electrical charge will flow to and away from the battery in accordance with diaphragm vibrations. By connecting a suitable charge flow sensing electrical circuit to the system, a usable voltage signal representation of the incident acoustical wave can be obtained.

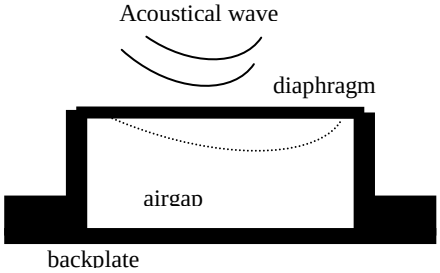


Figure 1. Cross-section of a MEMS-based capacitive type acoustical sensor

A parallel plate approximation is first considered to highlight the major aspects of the analysis (Figure 2).

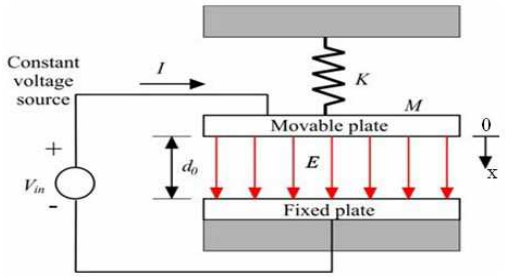


Figure 2. A simplified mechanical model of the MEMS with two parallel plates

The fixed plate of the capacitor with area A is connected with a constant supply voltage V. The other plate of the capacitor with mass m and area A is movable and rigid. The support of the moving plate is modeled through an equivalent spring with stiffness k. Without any electrostatic force, the gap between two plates of the capacitor in the MEMS is $d_0$. The coordinate x is shown in Figure 2 and the origin is at equilibrium without any voltage. By applying a voltage across the plates, an electrostatic attractive force $F_e(x)$ is induced which leads to a decrease of the gap spacing, thereby stretching the spring. This results in an increase of the mechanical elastic force (or spring force) $F_m(x)$ which counteracts the electrostatic force. Pull-in instability occurs as a result of the fact that the electrostatic force increases non-linearly with decreasing gap spacing, whereas the mechanical elastic force is a linear function of the change in the gap spacing. In simple terms, the pull-in voltage can be defined as the voltage at which the restoring spring force can no longer balance the attractive electrostatic force.
Neglecting any damping within the system, the equation of motion of the movable plate due to an electrostatic attraction force $F_e(x)$ caused by a constant supply voltage V is:

$$m\frac{d^2x}{dt^2} + kx = F_e(x) \tag{1}$$

The mechanical elastic force is $F_m(x) = kx$ and the capacitance of the movable-plate parallel-plate capacitor is given by :

$$C(x) = \frac{\varepsilon_0 A}{d_0 - x} \tag{2}$$

where $\varepsilon_0$ is the permittivity of the free space. The electrostatic attraction force $F_e(x)$ between the plates due to the charges on the plates can be found by differentiating the stored energy of the capacitor with respect to the position of the movable plate and is expressed as :

$$F_e(x) = \frac{d}{dx}\left(\frac{1}{2}V^2 C(x)\right) = \frac{\varepsilon_0 A V^2}{2(d_0 - x)^2} \tag{3}$$

At the static equilibrium the mechanical elastic force equals the electrostatic attraction force and the relationship between the voltage V and displacement of the movable plate is :

$$V=(d_0 - x)\sqrt{2kx/(\varepsilon_0 A)} \tag{4}$$

The maximum of the voltage is obtained for dV/dx=0 and from this equation we obtain the distance where the pull-in occurs:

$$dV/dx = -\sqrt{2k\,x/(\varepsilon_0 A)} + (d_0-x)k\sqrt{1/(2k\,x\,\varepsilon_0 A)} \quad (5)$$

The distance where the pull-in occurs is $x_{pi} = d_0/3$ and the pull-in gap is $d_{pi} = 2d_0/3$. The pull-in voltage for this ideal parallel plate structure is then :

$$V_{pi} = \sqrt{8kd_0^3/(27\varepsilon_0 A)} \quad (6)$$

and the spring constant of the movable plate is given by:

$$k = 27\varepsilon_0 A V_{pi}^3/(8\,d_0^3) \quad (7)$$

A graph of the normalized voltage as a function of the normalized displacement of the movable plate is shown in Figure 3. A stable displacement occurs for a normalized gap greater than 2/3 (or a normalized displacement of the movable plate smaller than 1/3).

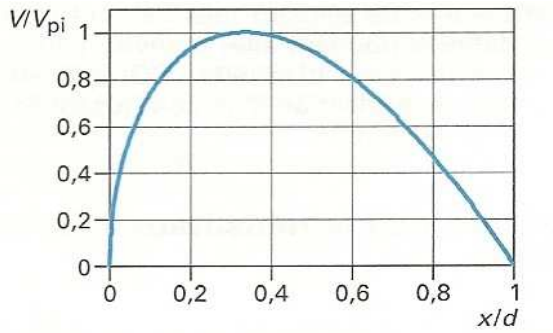


Figure 3. Variations of the normalized voltage for the electrostatic actuator

If the applied voltage is increased beyond the pull-in voltage, the resulting electrostatic force will overcome the elastic restoring force and will cause the movable plate to collapse on the fixed plate and the capacitor will be short circuited.

To obtain stiffness due to the electrostatic force we expand equation (1) using a Taylor series approximation about the nominal distance $x_0$ :

$$m\frac{d^2x}{dt^2} + \left(k - \frac{\varepsilon_0 A V^2}{(d_0-x_0)^3}\right)x = \frac{1}{2}\frac{\varepsilon_0 A V^2}{(d_0-x_0)^2}\left[1 - \frac{2x_0}{(d_0-x_0)}\sum_{n=3}^{N}\frac{n(x-x_0)^{n-1}}{(d_0-x_0)^{n-1}}\right] \quad (8)$$

The electrostatic attraction force effectively modifies the spring constant k of the movable plate and the effective spring constant at a specified voltage V is :

$$k_{effective} = \left(k - \frac{\varepsilon_0 A V^2}{(d_0-x_0)^3}\right) \quad (9)$$

The resonant frequency of the structure is shifted from $\omega_{res} = \sqrt{k/m}$ to $\omega_{res} = \sqrt{(k_{effective}/m}$ .

## 3 Deflection of a square diaphragm

Due to the presence of residual stress and a significantly large deflection of the diaphragm compared to its thickness, the developed strain energy in the middle of the diaphragm causes a stretch of the diaphragm middle surface. Figure 4 shows the principle of deflection of a diaphragm.

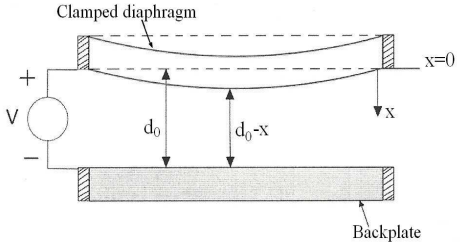


Figure 4. A schematic of electrostatic actuation

The deflection of the diaphragm middle surface corresponds to a nonlinear behavior of a rigidly clamped diaphragm and is known as spring hardening. Tabata et al [5] developed an analytical solution for the load-deflection of membranes. They found a relationship between the external load and the membrane deflection to determine the residual stress and Young's modulus of thin films. Pan et al [6] compared the analytical solution with FEM analysis. They found that the functional form of the analytical results is correct, but some constants have to be corrected. Pan et al also found that the analytical forms of the membrane's bending lines do not describe the real behavior very accurately. Maier-Schneider et al [7] found an analytical solution for the load-deflection behavior of a membrane by minimization of the total potential energy and assuming a functional form of the deflected membrane shape which extracted form [8]. The deflection of the midpoint of a square diaphragm under a uniform pressure load P can be expressed as [8] :

$$P(h_0) = C_1 \frac{e\sigma}{a^2} h_0 + C_2(\nu) \frac{eE}{a^4} h_0^3 \tag{10}$$

where P is the applied uniform pressure, $h_0$ the deflection of the diaphragm midpoint, e the diaphragm thickness, 2a the diaphragm side length, E the Young's modulus, $\nu$ the in-plane Poisson's ration and $\sigma$ the residual stress. The dimensionless constants $C_1$ and $C_2$ are numerical parameters which are obtained from [8]: $C_1$= 3,45 and $C_2(\nu) = 1{,}994(1\text{-}0{,}271\,\nu)/(1\text{-}\nu)$. The non-linear spring constant of the diaphragm is then :

$$k_{nl} = \frac{P(h_0)A}{h_0} = (C_1 \frac{e\sigma}{a^2} + C_2(\nu) \frac{e\hat{E}}{a^4} h_0^2) A \tag{11}$$

where $\hat{E} = E/(1-\nu^2)$ is the effective Young's modulus. The deflection-dependent nonlinearity due to spring hardening appears in equation (11) where the square of the midpoint deflection variable $h_0$ is considered. For a test device we consider the parameters given in table 1.

| parameter | e | a | $d_0$ | E | $\nu$ | $\sigma$ |
|---|---|---|---|---|---|---|
| value | 0,8 | 1,2 | 3,5 | 169 | 0,28 | 20 |
| unity | µm | µm | µm | GPa | - | MPa |

Table 1. Model parameters

A plot of the variations of the non-linear spring as a function of the deflection of the diaphragm midpoint is shown in figure 5. From this figure we can obtain the value of the non-linear spring. Note that this spring hardening has been obtained under the hypothesis of an applied uniform pressure.

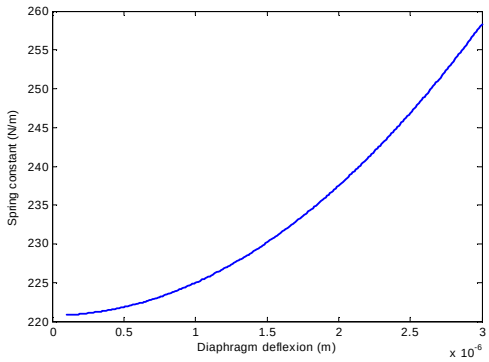


Figure 5. Spring constant and diaphragm deflection

The deflection of the diaphragm from mid-side to mid-side can be calculated from midpoint deflection $h_0$ as [8] :

$$h(y,0)= h_0\left[1+ 0{,}401\left(\frac{y}{a}\right)^2\right]\cos\left(\frac{\pi y}{2a}\right) \tag{12}$$

For a parallel plate configuration, the nonlinear electrostatic force is always uniform. However, for a rigidly clamped diaphragm, the electrostatic force becomes non-uniform due to a hemispherical deformation profile of the diaphragm (Figure 6). Thus, to evaluate the deflection of a rigidly clamped diaphragm under an electrostatic force, it is necessary to obtain a uniform linear model of the electrostatic force that can be applied in load-deflection equation (10).

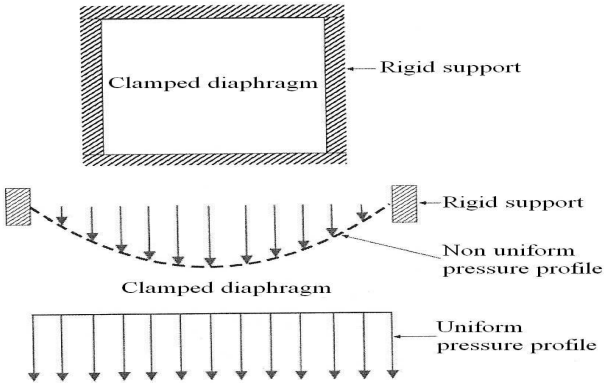


Figure 6. Non-uniformity of the pressure profile (top)
Unifomity of the pressure profile (bottom)

A uniform linearized model of the electrostatic force can be obtained from (8) by linearizing the electrostatic force about the zero deflection point x=0. We obtain then:

$$\varepsilon_0\, V^2\left(\frac{1}{2d_0^2}+\frac{x}{d_0^3}\right) A = k\, x \tag{13}$$

The left-hand of this equation equals an approximate uniform electrostatic force and the uniform electrostatic pressure on the diaphragm is :

$$P_{unif} = \varepsilon_0 \, V^2 \left( \frac{1}{2d_0^2} + \frac{x}{d_0^3} \right) \tag{14}$$

This equation is general and can be applied to any sort of diaphragms. The pull-in deflection is obtained for $x=d_0/3=h_0$ and the effective pull-in pressure is :

$$P(h_0) = C_1 \frac{e\sigma d_0}{3a^2} + C_2(\nu) \frac{e\hat{E} d_0^3}{27 a^4} = \frac{5\varepsilon_0 V_{pi}^2}{6 d_0^2} \tag{15}$$

and the pull-in voltage for the square clamped diaphragm is given by :

$$V_{pi} = \sqrt{\frac{6d_0^2}{5\varepsilon_0} \left[ \frac{C_1 e\sigma d_0}{3a^2} + \frac{C_2(\nu) e\hat{E} d_0^3}{27 a^4} \right]} \tag{16}$$

Figure 7 shows the variations of electrostatic and elastic forces as a function of the displacement x, obtained from (13). The spring constant k is obtained using equation (11) or Figure 5. At a distance of one-third of the original airgap, the elastic force graph intersects the 17.45 volts constant voltage graph and thus gives the voltage where the pull-in occurs.

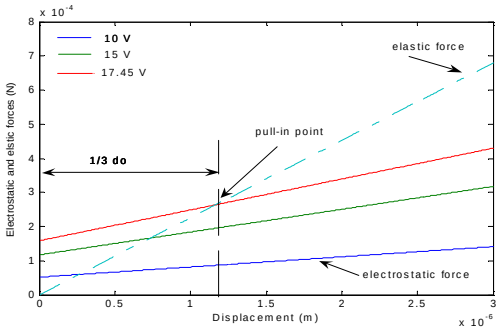


Figure 7. Electrostatic and elastic forces

The pull-in voltage can be calculated using equation (16). If we use equation (6) we obtain $V_{pi}$ = 15.02 volts, a value which is 2.43 volts smaller than the value obtained with the method proposed in this work. The mid-side to mid-side deflection profiles of the diaphragm for different voltages is shown in figure 8.

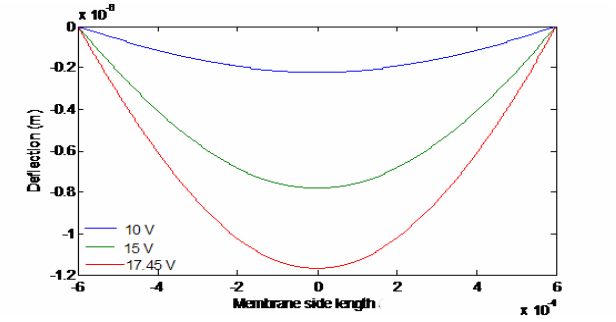


Figure 8. Mid-side to mid-side deflection profiles of a clamped square diaphragm

Figure 9 shows the pull-in voltage as a function of the airgap thickness. For a value of $d_0 = 3.5\,\mu m$ we obtain the pull-in voltage of 17.45 volts.

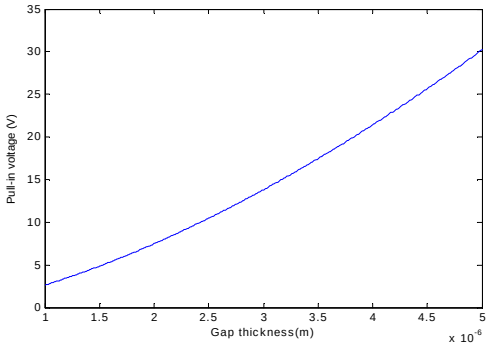


Figure 9. Tension of collapse for a clamped square diaphragm

## 4 Deflection of a circular diaphragm

The analytical method developed in the preceding section to determine the pull-in voltage for a rigidly clamped square diaphragm can be adopted to evaluate the pull-in voltage for a circular diaphragm under electrostatic load. Figure 10 shows a clamped circular diaphragm of radius a and thickness e under a uniform transverse load P.

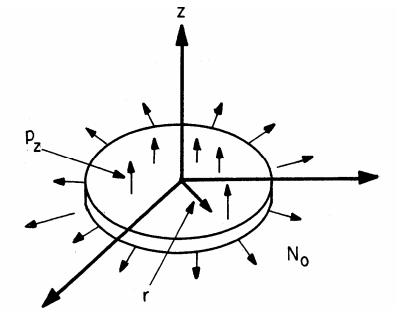


Figure 10. Schematic of a clamped circular diaphragm

For a rigidly clamped circular diaphragm the deflection of the midpoint of the diaphragm under a uniform pressure P can be expressed as [9] :

$$h(r)= \frac{12(1-\nu^2)Pa^4}{T^2 E e^3}\left[\frac{I_0(T r/a)-I_0(T)}{2\,T\,I_1(T)}+\frac{a^2-r^2}{4a^2}\right] \qquad (17)$$

where r is the radial position, h(r) the defection at a radial position r, T the tension parameter, $I_0$ and $I_1$ are the modified function Bessel functions of first kind of zeroth and first order respectively. The tension parameter is defined as:

$$T = \frac{a}{e}\sqrt{\frac{12(1-\nu^2)\sigma}{E}} \qquad (18)$$

The deflection of the center of the diaphragm is obtained from equation (17):

$$h_0 = \frac{12(1-\nu^2)Pa^4}{T^2 E e^3}\left[\frac{1}{4} - \frac{I_0(T)}{2T I_1(T)}\right] \tag{19}$$

and we obtain the applied pressure $P(h_0)$ in the format of equation (15) :

$$P(h_0) = \frac{T^2 E e^3 h_0}{12(1-\nu^2)a^4}\left[\frac{1}{4} - \frac{I_0(T)}{2T I_1(T)}\right]^{-1} \tag{20}$$

Using the same method as the square diaphragm case, and considering $h_0$ in the pull-in deflection ($h_0=d_0/3$) we obtain then :

$$\frac{5\varepsilon_0 V_{pi}^2}{6 d_0^2} = \frac{T^2 E e^3 d_0}{36(1-\nu^2)a^4}\left[\frac{1}{4} - \frac{I_0(T)}{2T I_1(T)}\right]^{-1} \tag{21}$$

And the expression for the pull-in voltage for a rigidly clamped circular diaphragm is :

$$V_{pi} = \sqrt{\frac{T^2 E e^3 d_0^3}{30\varepsilon_0(1-\nu^2)a^4}\left[\frac{1}{4} - \frac{I_0(T)}{2T I_1(T)}\right]^{-1}} \tag{22}$$

Figure 11 shows the pull-in voltage for a range of diaphragm radius.

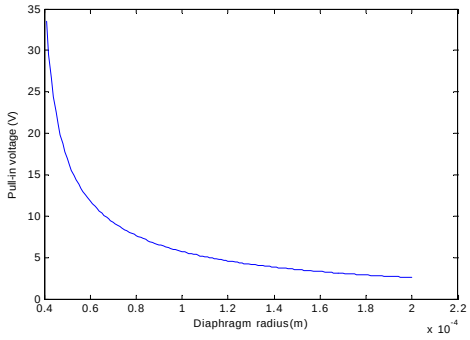


Figure 11. Pull-in voltage for clamped circular diaphragms

Equation (22) provides a model that includes spring-hardening phenomena and a linearized approximation to the nonlinear electrostatic force, resulting in a more accurate determination of the pull-in voltage for circular diaphragms.

## 5 Conclusion

A new relatively simple closed-form model to evaluate the pull-in voltage associated with a rigidly clamped square or circular diaphragm subject to an electrostatic force has been developed. The method incorporates the nonlinear and non uniform nature of the electrostatic force associated with a clamped diaphragm deformation. However, the approach is based on a linearized uniform approximation of the nonlinear electrostatic force due to a voltage an the use of a 2D load deflection model. The spring hardening effect associated with deflection of a clamped diaphragm has been evaluated. The method can be extended to determine the pull-in voltage for other microstructures such as cantilever beams under electrostatic excitation.

**References**

[1] Senturia S., Microsystem Design, Springer (2000)

[2] Puers R, Lapadatu D., Electrostatic forces and their effects on capacitive mechanical sensors, *Sensors and Actuators A*, 56, 203-210 (1996)

[3] Chowdhury S., Ahmadi M. , Miller W.C., A new analytical model for the pull-in voltage of clamped diaphragms subject to electrostatic force, *Sensor Letters*, 2, 106-112 (2004)

[4] Chowdhury S., Ahmadi M. , Miller W.C., A closed form model the pull-in voltage of electrostatically actuated cantilever beams, *Journal of Micromechanics and Microengineering*, 15, 756-763 (2005)

[5] Tabata S., Kawahata K., Sugiyama S, Igarashi I., Mechanical property measurements of thin films using load-deflection of composite rectangular membranes, *Sensors and Actuators*, 20, 135-141 (1989)

[6] Pan J.Y., Lin P., Maseeh F., Senturia S.D., Verification of FEM analysis of load-deflection methods for measuring mechanical properties of thin films, *IEEE Solid-State Sensors and Actuators Workshop*, Hilton Head, (1990)

[7] Maier-Schneider D., Maibach J, Obermeier E., A new analytical solution for the load-deflection of square membranes, *Journal of Microelectromechanical Systems*, 4, 238-241 (1995)

[8] Timoshenko S., Theory of Plates and Shells, Mac Graw Hill (1959)

[9] Sheplak M., Seiner J.M., A MEMS microphone for aeroacoutics measurements, *37th AIAA Aerospace Sciences Meeting, Reno* (1999)